BIOCHEMISTRY
including biophysical chemistry & molecular biology

Article

pubs.acs.org/biochemistry

Antimicrobial Peptide LL-37 Is Both a Substrate of Cathepsins S and K and a Selective Inhibitor of Cathepsin L

Pierre-Marie Andrault,[†] Sergey A. Samsonov,[‡] Gunther Weber,[§] Laurent Coquet,[∥] Kamran Nazmi,[⊥] Jan G. M. Bolscher,[⊥] Anne-Christine Lalmanach,[#] Thierry Jouenne,[∥] Dieter Brömme,[○] M. Teresa Pisabarro,[‡] Gilles Lalmanach,[†] and Fabien Lecaille*[,†]

[†]INSERM, UMR 1100, Pathologies Respiratoires: protéolyse et aérosolthérapie, Centre d'Etude des Pathologies Respiratoires, Equipe 2: "Mécanismes Protéolytiques dans l'Inflammation", Université François Rabelais, F-37032 Tours cedex, France

[‡]Structural Bioinformatics, BIOTEC TU Dresden, Tatzberg 47-51, 01307 Dresden, Germany

[§]INSERM, UMR 1069, Nutrition Croissance et Cancer, Université François Rabelais, F-37032 Tours cedex, France

[∥]CNRS UMR 6270, Plate-forme de Protéomique "PISSARO" de l'IRIB, Université de Rouen, F-76821 Mont-Saint Aignan, France

[⊥]Department of Oral Biochemistry, Academic Centre for Dentistry Amsterdam, University of Amsterdam and VU Universiteit Amsterdam, 1081 LA, Amsterdam, The Netherlands

[#]INRA, UMR 1282 Infectiologie et Santé Publique, Université François Rabelais, F-37380 Nouzilly, France

[○]Department of Oral Biological and Medical Sciences, The University of British Columbia, Vancouver, British Columbia V6T1Z3, Canada

ABSTRACT: Lung cysteine cathepsins B, K, L, and S contribute to physiological and pathological processes including degradation of antimicrobial peptides/proteins (AMPs) such as surfactant protein SP-A, lactoferrin, secretory leukocyte peptidase inhibitor, and beta-defensins-2 and -3. Substantial amounts of uncleaved LL-37, a 37-mer cationic AMP, were observed in the sputum of patients with cystic fibrosis (CF). Nevertheless LL-37 was degraded after prolonged incubation in CF sputum, and the hydrolysis was blocked by E-64, a selective inhibitor of cysteine proteases. Cathepsins K and S, expressed in human alveolar macrophages, thoroughly hydrolyzed LL-37 *in vitro*, whereas it competitively inhibited cathepsin L (K_i = 150 nM). Cleavage of LL-37 by cathepsins S and K impaired its antimicrobial activity against *Pseudomonas aeruginosa* and *Staphylococcus aureus*, in a time- and concentration-dependent manner. The exchange of residues 67 and 205 in the S2 pockets of cathepsins L (Leu67Tyr/Ala205Leu) and K (Tyr67Leu/Leu205Ala) switched the specificity of these mutants toward LL-37. Molecular modeling suggested that LL-37 interacted with the active site of cathepsin L in both forward (i.e., substrate-like) and reverse orientations with similar binding energies. Our data support the hypothesis that cysteine cathepsins modulate the innate immunity response by degrading distinct and representative members of the AMP family.

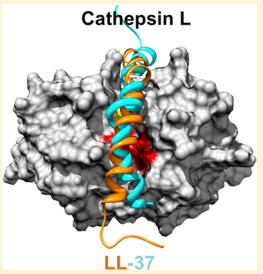

The human airway epithelium is constantly exposed to a myriad of potential airborne pathogens and therefore constitutes an essential frontline of the host defense against infections. To prevent microbial colonization, the lung epithelial lining fluid displays an arsenal of effective antimicrobial proteins and polypeptides (AMPs) that include larger proteins such as lysozyme, lactoferrin, surfactant proteins, the secretory leukocyte protease inhibitor (SLPI), as well as cationic peptides such as human β-defensins (hBD) and cathelicidin LL-37. In addition to their broad-spectrum antimicrobial activity against a range of bacteria, fungi, and viruses, AMPs play a key role in the modulation of innate and adaptive immunity and in wound repair (for review, see refs 1 and 2). However, the activity of some AMPs, such as SLPI, hBD-2 and -3, SP-A, and LL-37, may be impaired in airway inflammatory diseases like cystic fibrosis (CF) due to their susceptibility to proteolytic degradation by opportunistic pathogens including *Pseudomonas aeruginosa* and *Staphylococcus aureus* as well as by host proteases.[3−5] LL-37 activity may also be impaired in CF due to interactions with anionic filamentous (F)-actin,[6] DNA,[7] glycosaminoglycans,[8,9] and mucins,[10] which inhibit its antimicrobial activity and protect it from proteolysis. Indeed, an elevated concentration of LL-37, reaching levels of 15 μg/mL, is observed in the bronchoalveolar lavage fluid of CF patients and is correlated with pulmonary inflammation and disease severity.[11,12] Thus, the regulation of LL-37 during the pathogenesis of CF lung disease remains unclear and needs further investigation.

The only cathelicidin in humans is expressed as a 18-kDa precursor (hCAP18) that is expressed by various cell types (e.g., leukocytes, epithelial cells) and found in body fluids (e.g., BALF, saliva, plasma). hCAP18 consists of a highly conserved N-terminal prodomain (the cathelin-like domain, i.e., hCLD) and a cationic C-terminal domain that corresponds to LL-37.[13] After secretion, the precursor is cleaved by kallikreins produced

Received: March 4, 2015
Revised: April 13, 2015
Published: April 17, 2015

DOI: 10.1021/acs.biochem.5b00231
Biochemistry 2015, 54, 2785−2798

in keratinocytes[14] and proteinase 3 from neutrophils[15] to generate LL-37. It is noteworthy that the lack of activation of proteinase 3 leads to an accumulation of hCAP18 in the gingiva and saliva of patients with Papillon−Lefèvre syndrome, favoring infection by pathogenic bacteria.[16] Despite a cystatin-like fold, the cathelin-like domain possesses no apparent inhibitory activity against cysteine cathepsin L (CatL).[17] Conversely, both LL-37 and hCAP18 reduce CatL activity in a dose-dependent manner, suggesting that the C-terminal of hCAP18 is critical in the inhibition. The positive charge and amphipathic α-helical secondary structure of LL-37 allow it to interact with negatively charged phospholipids of bacteria membrane, resulting in their permeabilisation by the formation of transmembrane pores and thus leading to bacterial lysis.[18] Although the antimicrobial activity of LL-37 supports its potential use as a therapeutic agent against bacterial infection and inflammatory diseases, its effectiveness could be limited by specific proteases present in the CF lung.[19,20] We and others reported that hBD-2 and -3, SLPI, lactoferrin, and SP-A are cleaved and inactivated in CF lungs by human cysteine cathepsins B, L, and S (CatB, L, and S).[21−24] Cysteine cathepsins are produced by lung macrophages, fibroblasts, and epithelial cells and participate primarily in intracellular proteolytic pathways (for review, see ref 25). Cathepsins are also found to be extracellularly active as membrane-bound and soluble forms and contribute with other proteases to a variety of pathophysiological processes (for review, see refs 26 and 27). Overall, these observations raised the question whether LL-37 is an inhibitor, a substrate, or combines both functions toward cathepsins. Here, we evaluated the potential of CatB, K, L, and S to inactivate the antimicrobial function of LL-37 against Gram-negative and Gram-positive bacteria. Furthermore, we investigated the molecular mechanism of the inhibition of CatL by biochemical and molecular modeling studies.

EXPERIMENTAL PROCEDURES

Enzymes. Human Cats B, L, and S were supplied by Calbiochem (VWR International S.A.S., France). Human CatK, S2 cathepsin L-like (Tyr67Leu/Leu205Ala) mutant of CatK and S2 cathepsin K-like (Leu67Tyr/Ala205Leu) mutant of CatL were produced as described previously.[28] Human neutrophil elastase (HNE) was purchased from BioCentrum (Krakow, Poland). Active site concentrations of cathepsins were determined using L-3-carboxy-trans-2,3-epoxy-propionyl-leucylamide-(4-guanido)-butane (E-64) (Sigma-Aldrich, Saint-Quentin Fallavier, France). HNE titration was performed with α1-antitrypsin (Boehringer Ingelheim, Reims, France) as previously described.[29]

Substrates and Synthetic Inhibitors. Benzyloxycarbonyl-Phe-Arg-7-amino-4-methyl coumarin (Z-Phe-Arg-AMC) was purchased from Bachem (Bachem Biochimie, Voisin-le-Bretonneux, France). PMSF, pepstatin A, EDTA, AEBSF (Pefabloc), and MMTS were from Sigma-Aldrich. *N*-(L-3-*trans*-Propylcarbamoyloxirane-2-carbonyl)-L-isoleucyl-L-proline (CA-074) and DTT (DL-dithiotreitol) were from Calbiochem (VWR International S.A.S., France). Morpholinourea-leucinyl-homophenylalanine-vinyl-sulfone phenyl inhibitor (LHVS) was a kind gift from Dr. J. H. McKerrow (University of California, San Diego, La Jolla, CA, USA). Glycosaminoglycans: chondroitin 4-sulfate (C4-S) from bovine trachea (MW approx: 20−30 kDa), low molecular weight heparin (HP) from porcine intestinal mucosa (MW: 15−17 kDa), heparan sulfate (HS) from bovine kidney (MW approx: 14 kDa), hyaluronic acid (HA) from Streptococcus equi (MW: 1400 kDa) were from Sigma-Aldrich. Purified GAGs were diluted in 0.1 M sodium acetate buffer, pH 5.5 at 3 mg/mL. All other reagents were of analytical grade.

Synthetic Peptides. Unless otherwise stated, all peptides were of L-configuration. LL-37 (LLGDFFRKSKEKIGKEFKRIVQRIKDFLNLRVPRTES), D-LL-37 (amino acids were of D-configuration) and scrambled LL-37 (Sc-LL-37: RSLEGTDRFPFVRLKNSRKLEFKDIKGIKREQFVKIL) were purchased from GeneCust (GeneCust Europe, Dudelange, Luxembourg). Synthesis of truncated forms of LL-37 is detailed elsewhere.[30] The individual sequences are LL-31, LLGDFFRKSKEKIGKEFKRIVQRIKDFLRNL; LL-25, LLGDFFRKSKEKIGKEFKRIVQRIK; LL-19, LLGDFFRKSKEKIGKEFKR; LL-13, LLGDFFRKSKEKI; RK-25, RKSKEKIGKEFKRIVQRIKDFLRNL; IG-19, IGKEFKRIVQRIKDFLRNL; RK-19, RKSKEKIGKEFKRIVQRIK; IG-13, IGKEFKRIVQRIK; RK-31, RKSKEKIGKEFKRIVQRIKDFLRNLVPRTES; IG-25, IGKEFKRIVQRIKDFLRNLVPRTES; RI-19, RIVQRIKDFLRNLVPRTES; KD-13, KDFLRNLVPRTES. SE-37 (the reverse peptidyl sequence of LL-37, i.e., SETRPVRLNLFDKIRQVIRKFEKGIKEKSKRFFDGLL) and biotin-LC-LL-37 were from Anaspec (Eurogentec, Angers, France). DF-22 (DFFRKSKEKIGKEFKRIVQRIK) was synthesized as a peptidyl amide by Fmoc-solid-phase chemistry and purified according to ref 31.

Ethics Statement. The Institutional Review Board of the French Learned Society for Respiratory Medicine (Société de Pneumologie de Langue Française) approved the study, and written informed consent was obtained from the participants to the study (Biocollection DC 2010-1216, CHU Tours). Clinical charts and functional records were collected on a standardized and anonymous collection form. An adult patient suffering from inflammatory pulmonary disease was submitted to a routine bronchoalveolar lavage procedure (Department of Pneumology, CHRU Bretonneau, The University Hospital, Tours, France) with respect to recommendations of the local institutional Ethical Committee, as reported elsewhere.[32] CF sputum samples were collected on a routine basis from adult patients followed at the Teaching Hospital of Besançon (CHU Jean Minjoz, France) between 2009 and 2010 as detailed previously.[33]

Sputum Samples from CF Patients. Six expectorated sputum samples (three *P. aeruginosa*-positive and three *P. aeruginosa* negative samples named Ps+ and Ps-, respectively) were obtained from CF adult patients and were kindly provided by Dr. G. Couetdic and Dr. P. Plésiat (Laboratoire de Bactériologie, CHU Jean Minjoz, Besançon, France). Samples were considered as "waste", and subsequently the protocol used for this study did not need a specific agreement from the local research ethics committee. Following the protocol as previously described,[33] each Ps+ and Ps− samples sample was instantly suspended in the conservative buffer A: 100 mM sodium acetate, pH 5.0 containing a serine, asparatate, metallo, and cysteine protease inhibitor cocktail (0.5 mM PMSF, 0.5 mM EDTA, 40 μM pepstatin A, and 1 mM MMTS) and centrifuged at 5000*g* at 4 °C for 10 min. The supernatant was frozen and stored at −80 °C until required for analysis. Bicinchoninic acid assays were used to determine the protein concentrations in supernatants (BCA protein assay kit, Interchim, Montluçon, France). To restore the activity of cathepsins, samples were incubated in 100 mM acetate sodium, pH 5.5, DTT 5 mM, Brij35 0.01% (buffer B) for 30 min. The presence of sulfated GAGs in CF sputum (30 μg total protein) was determined

DOI: 10.1021/acs.biochem.5b00231
Biochemistry 2015, 54, 2785−2798

using 1,9-dimethylmethylene blue (Sigma-Aldrich) staining method and quantified by spectrophotometry at 520 nm.

Western Blot Analysis of LL-37, HBD-2, and SP-A in CF Sputum. The polyclonal anti-LL-37 antibody was purchased from Innovagen (Lund, Sweden) and the polyclonal anti-hBD-2 antibody from Research Diagnostic Inc. (Flanders, New Jersey, USA). The polyclonal anti-SP-A antibody was a kind gift from Dr. Henk Haagsman (Utrecht University, Netherlands). Recombinant hBD-2 was purchased from Research Diagnostic Inc., and purified human SP-A was a kind gift from Dr. Ruud Veldhuizen (University of Western Ontario, Ontario, Canada). Supernatants of CF sputum (standardized amount: 30 μg protein/sample) were diluted in Laemmli buffer under reducing conditions and boiled for 5 min. Finally, samples were loaded onto 20% polyacrylamide gel for the detection of LL-37 and hBD-2, or on 12% gels for the detection of SP-A, and electrophoretically separated under reducing conditions (Bio-rad System). Prestained molecular mass standards (low molecular range) were obtained from Sigma-Aldrich. For Western blot analysis, gels were electroblotted onto nitrocellulose membranes (Hybond-ECL, Amersham Biosciences, Buckinghamshire, UK). Membranes were incubated under agitation overnight at 4 °C with anti-LL-37 antibody (1:10000 in PBS, 0.1% Tween 20, 5% powdered milk), then incubated with secondary IgG-horseradish peroxidase conjugate (1:5000) for 1 h at room temperature prior to the detection using the ECL Plus Western Blotting Detection system (Amersham Biosciences). A similar protocol was used for the anti-SP-A (1:2500) and anti-hBD-2 antibodies (1:5000). LL-37 (10 ng), SP-A (150 ng), and hBD-2 (10 ng) were used as controls.

Hydrolysis of LL-37 in CF Sputum. Ps+ supernatants were incubated (1−6 h) at 37 °C in 100 mM acetate sodium, pH 5.5, 5 mM DTT, Brij35 0.01% (buffer B) (final volume: 16 μL; 30 μg of protein). Reaction mixtures were stopped with Laemmli buffer and boiled for 3 min. Controls were performed in the presence of E-64 (10 μM). Samples were subjected to SDS-PAGE (20%) under reducing conditions and then immunoblotted as described above using an anti-LL-37 antibody.

Hydrolysis of LL-37 by Human Alveolar Macrophages. Alveolar macrophages were obtained from a bronchoalveolar lavage fluid (BALF) of a nonsmoking and nonfibrotic patient. BALF was centrifuged at 129*g* for 5 min, and the cell pellet was resuspended in RPMI 1640 media supplemented with 1% heat-inactivated fetal calf serum and 1% penicillin/streptomycin. Adherent cells were cultured for 24 h at 5% CO_2 and 37 °C. Culture media was replaced and macrophages were grown for additional 24 h without fetal calf serum. Culture media from macrophages were harvested and treated immediately in 100 mM sodium acetate, pH 5.0, 0.5 mM PMSF, 0.5 mM EDTA, 40 μM pepstatin A, and 1 mM MMTS (buffer A). The supernatants were centrifuged for 5 min at 9000*g* at 4 °C to remove floating cells and concentrated by centrifugation with Vivaspin 4 concentrators (Sartorius) at 4000*g* for 30 min. Alternatively macrophage layers were washed once in ice-cold PBS and scrapped off in the buffer A. Total cell extracts were obtained by a series of three freeze/thaw cycles in liquid nitrogen and a 37 °C water bath. Lysate was centrifuged at 5000*g* at 4 °C for 10 min. Supernatants were collected, and cell pellets were resuspended in 150 μL of the conservative buffer A. Measurement of the overall cathepsin activity was performed using Z-FR-AMC (50 μM) in buffer B at pH 5.5. Total cathepsin activity was determined by titration with E-64. LL-37 (30 ng) was incubated for 0−24 h in the reactive buffer B with supernatants, cytosolic fractions, and cell-free membrane fractions. In parallel, samples were preincubated with E-64 (10 μM), CA-074 (10 μM), and Mu-Leu-Hph-VSPh (100 nM) prior to adding LL-37. Samples were subjected to SDS-PAGE (20%) under reducing conditions and then immunoblotted using an anti-LL-37 antibody.

Hydrolysis of LL-37 and LL-37-Derived Peptides by Cathepsins. LL-37, D-LL-37, scrambled LL-37, and SE-37 (89 μM) were incubated at different incubation times (10−240 min) in the presence or absence of purified CatB, K, L, or S (5−89 nM) in 100 mM sodium acetate buffer pH 5.5, containing 2 mM DTT and 0.01% Brij35 (buffer C) at 37 °C. Similar experiments were performed with the human S2 subsite CatL variant (Leu67Tyr/Ala205Leu) and the human S2 subsite CatK variant (Tyr67Leu/Leu205Ala). LL-37 (89 μM) was incubated with CatK and S (5 nM) in the presence or absence of chondroitin 4-sulfate (C4-S), heparan sulfate (HS), hyaluronic acid (HA), and heparin (HP) (0.0015−0.15%) in the reactive buffer (pH 5.5). Control experiments were performed in the presence of E-64 (10 μM). Alternatively hydrolysis of LL-37 was performed in the presence of CatS in 100 mM sodium phosphate buffer, pH 7.4, containing 2 mM DTT and 0.01% Brij35. Hydrolysis of LL-37 by HNE was performed in 50 mM HEPES buffer, pH 7.4, 0.05% NP40, 150 mM NaCl. Inhibition control of HNE was performed with 10 μM Pefabloc. Reaction mixtures were boiled in Laemmli buffer for 3 min and loaded onto 8−25% precast gradient gels (Pharmacia, Phastgel, GE Healthcare Europe, Paris, France). Gels were stained with Coomassie Brillant Blue G-250. The ImageJ software (NIH, Bethesda, MD, USA) was used for densitometric analysis of LL-37 peptide band.

Identification of LL-37 Cleavage Sites. Each cathepsin (20 nM, final concentration) was incubated with LL-37 (89 μM) at different times (30−240 min) in 100 mM sodium acetate buffer pH 5.5, containing 2 mM DTT and 0.01% Brij35 (buffer C) at 37 °C. The same experiments were carried out with D-LL-37, sc-LL-37, SE-37, LL-25, LL-19, LL-13, RK-25, IG-19, RK-19, IG-13, RK-31, IG-25, RI-19, and KD-13 (89 μM final). The reaction was stopped by adding ethanol (1:5, v/v) (Carlo Erba Reagents, Val de reuil, France). After centrifugation at 3200*g* for 30 min at 4 °C, the precipitate was removed, and the supernatant containing the native peptide and/or its proteolytic fragments was evaporated to dryness and redissolved in 0.1% trifluoroacetic acid. An aliquot of each sample was analyzed by reverse-phase high-performance liquid chromatography (RP-HPLC) with a C-18 column (RP-18, LichroCART, Purospher, Merck, France) using a linear 0−90% water/acetonitrile gradient in the presence of 0.1% TFA, at a flow rate of 0.5 mL/min. Chromatograms were treated with ChromQuest software (SpectraSystem). Fragments were collected and analyzed by MALDI-TOF mass spectrometry using a MALDI-TOF-TOF Ultraflex (Bruker Daltonics). Calibration was performed with peptides of known molecular mass (1−2.5 kDa range). The accuracy of mass determinations was ±0.02%. The identification of LL-37 cleavage sites was determinated with the FindPept Tool accessible to SIB Bioinformatics Resource Portal (http://web.expasy.org/cgi-bin/findpept/findpept_form.pl).

Antimicrobial Activity. LL-37 (200 μM) was incubated in the presence or absence of each cathepsin (11−44 nM) in buffer C for 1−6 h at 37 °C. Control experiments were conducted with heat-inactivated cathepsins. After incubation, an

DOI: 10.1021/acs.biochem.5b00231
Biochemistry 2015, 54, 2785−2798

aliquot was taken from each sample and diluted 1:2, 1:5, 1:10, and 1:20 in the reactive buffer. Samples were then precipitated with absolute ethanol and centrifuged at 3200*g* for 30 min at 20 °C. Supernatant containing LL-37 and/or its proteolytic fragments were evaporated, and the dried pellets were resuspended in 10 μL of sterilized ultrapure water. Antimicrobial activity of each sample was then evaluated by radial diffusion assay technique (RDA) as previously described.[34] Briefly, bacterial strains *E. coli* J5 (ATCC 43745), *P. aeruginosa* (ATCC 25010), and *S. aureus* (ATCC 29740) were grown overnight in 2 mL of fresh TSB at 37 °C under gentle agitation. Absorbance of culture was then measured at 620 nm. On the basis of the relationship Abs_{620} 1 = 2.5 × 10^8 CFU/mL[34] culture was diluted to obtain a bacterial concentration of 5 × 10^6 CFU/mL in 50 mL of fresh TSB and then incubated for an additional 2.5 h at 37 °C under gentle agitation to obtain a mid logarithmic phase organism. Bacteria were then centrifuged at 900*g* for 10 min at 4 °C and washed once with cold 10 mM sodium phosphate buffer, pH 7.4 and resuspended in 10 mL of the same buffer. Bacterial strains (4 × 10^6 CFU/mL) were added to 10 mL of previously autoclaved warm poor tryptone soy agar (TSA) (tryptone soy powder: 0.03%, LE agarose: 0.8%) maintained in liquid phase. Poor TSA containing bacteria was then poured in an 85 mm diameter Petri dish (Corning, New York, USA) to form a uniform layer. A 2.5 mm diameter gel punch was used to make wells. After 6 μL was added to each sample per well, plates were incubated at 37 °C for 3 h to allow radial diffusion and then overlaid with 10 mL of rich TSA (TS powder: 12%, LE agarose: 1%). After an overnight incubation, the diameter of bacterial growth inhibition (expressed in mm) was measured and subtracted from the diameter of the well. Antimicrobial activity of synthetic DF-22 and RK-19 was assessed following the same protocol. Minimal inhibitory concentration (MIC) of LL-37 was determined by plotting the diameter of bacterial growth inhibition against the log of peptide concentration (20−400 μM). The intersection of the slope with the *x*-axis represents the lowest concentration of peptide that totally inhibits visible bacterial growth. The same experiments were carried out with DF-22 and RK-19. Assays were performed in triplicate and repeated twice.

Bactericidal Activity. Bactericidal activity of LL-37, DF-22, and RK-19 was assessed using Live/Dead BacLight bacterial viability Kit (Molecular Probes, InVitrogen Life Technologies SAS, Saint Aubin, France) as previously described.[24] Briefly, each peptide (concentration = 1 × MIC) was added to log-phase *P. aeruginosa* (2 × 10^8 CFU/mL) or *S. aureus* (2 × 10^6 CFU/mL), and samples were incubated for 3 h at room temperature. Fluorescence of both membrane-permeable SYTO 9 fluorophore that labels live bacteria and membrane-impermeable propidium iodide was measured following manufacturer's instructions. The experiments were performed in triplicate, and viability data were averaged.

CD Spectroscopy. CD spectra of LL-37, DF-22, and RK-19 were obtained using a Jasco J-810 spectropolarimeter (Jasco France, Bouguenais, France) equipped with a Peltier thermostat system. The path length of the cell was 1 mm (Hellma, VWR). Peptide concentration was 20 μM. Data acquisitions were made at 0.1 nm intervals with a dwell time of 1 s between 200 and 260 nm, at 37 °C in 100 mM sodium phosphate buffer pH 5.5 and pH 7.4, and averaged from three repeated scans. Similar assays were performed in aqueous solution. Secondary structure content was assessed by deconvolution of the CD spectra using spectra manager software (Jasco). Prediction of secondary structure and determination of helicity were performed using the Agadir program (http://agadir.crg.es). Calculated mean hydropathicity was based on the hydrophobicity scales for amino acids.[35]

Inhibition of CatL by LL-37. CatL (2 nM) was incubated with LL-37 (0−900 nM) in 96-well microtitration plates (Nunc microtiter plates, ThermoFisher Scientific, France) in 100 mM sodium acetate buffer pH 5.5, containing 2 mM DTT and 0.01% Brij35 (buffer C) at room temperature. After addition of Z-Phe-Arg-AMC (2.5 to 20 μM), the residual peptidase activity was followed at 37 °C by monitoring the fluorescence release (Spectramax Gemini spectrofluorimeter, Molecular Devices, Bioproducts) (wavelengths of 350 nm for excitation and of 460 nm for emission). Similar assays were performed with CatB, K, and S. In addition, experiments were performed with D-LL-37, sc-LL-37, SE-37, LL-25, LL-19, LL-13, RK-25, IG-19, RK-19, IG-13, RK-31, IG-25, RI-19, and KD-13 (900 nM). The type of inhibition and K_i values were determined using Lineweaver−Burk plots ($1/S = f(1/v)$) and Dixon plots ($1/v = f([I])$), respectively. Furthermore, CatL peptidase activity was monitored at 37 °C in the presence of LL-37 (900 nM) using buffer C supplemented with increasing concentration of NaCl (0 to 1 M). The ability of LL-37 to interact with the S2 CatL and S2 CatK variants was measured using Z-Phe-Arg-AMC as substrate. Assays were performed at least in three individual experiments in triplicate, and all data were treated with SoftMax Pro software (Molecular Devices). The values represent means ± SD.

Computational Analysis. The following PDB structures were used: CatK (PDB ID: 3KWZ, 1.49 Å), CatL (PDB ID: 2XU4, 1.12 Å), proCatK (PDB ID: 1BY8, 2.60 Å), and LL37 (PDB ID: 2K6O, NMR). Docking of LL-37 to CatK and L was carried out with ClusPro 2.0.[36] MD simulations were carried out using AMBER 11.[37] Docked complexes were simulated in a TIP3P water truncated octahedron periodic box with the minimal distance of 8 Å from the solute atoms to the box boundary and neutralized by counterions. Molecular dynamics (MD) simulations were preceded by two energy-minimization steps: 500 cycles of steepest descent and 1000 cycles of conjugate gradient with 10 kcal/mol Å harmonic restraints on protein atoms; 3000 cycles of steepest descent and 3000 cycles of conjugate gradient without constraints; 10 ps of heating of the system from 0 to 300 K; 100 ps of MD equilibration at 300 K and 10^6 Pa in isothermal isobaric ensemble (NPT). Ten ns of MD were carried out in periodic boundary conditions in NPT ensemble with Langevin temperature coupling with collision frequency parameter γ = 1 ps^{-1} and Berendsen pressure coupling with a time constant of 1.0 ps. The SHAKE algorithm, a 2 fs time integration step, an 8 Å cutoff for nonbonded interactions and the Particle Mesh Ewald method were used. ff99SB force field parameters were used. Postprocessing energetic analysis was carried out in a continuous solvent model using molecular mechanics-generalized Born surface area (MM-GBSA) with igb = 2 for each 50th frame (100 frames in total). In order to calculate individual impacts of LL-37 residues to the binding of CatL in the analyzed docking poses, MM-GBSA calculations of per residue free energy decomposition were carried out using default parameters. To obtain estimates for the binding energy of LL-37 truncated peptides in both poses, the energy values obtained for each amino acid value of the truncated peptides were summed up. This approach should be cautionally interpreted as it is based on the assumption that truncated mutants specifically interact in a similar manner as to

DOI: 10.1021/acs.biochem.5b00231
Biochemistry 2015, 54, 2785−2798

the corresponding parts of the full LL-37 peptide. Statistical analysis of modeling data was carried out with the R package.[38]

Statistical Analysis. Statistical significance was assessed using the nonparametric two-way Mann−Whitney U test. A *p*-value of less than 0.05 was considered statistically significant.

RESULTS

Detection of LL-37 in Human CF Sputum. Immunoreactive LL-37 (4.5 kDa) was present in both *P. aeruginosa* positive (Ps+) and negative (Ps-) CF expectorations samples (Figure 1A). According to densitometric analysis, the estimated

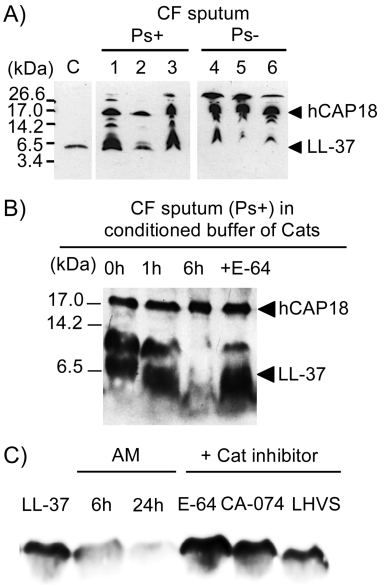

Figure 1. Degradation of LL-37 by human cathepsins in CF sputum supernatants and alveolar macrophages. (A) Status of LL-37 in cell-free supernatants of *P. aeruginosa*-positive (Ps+, samples: 1−3) and negative (Ps−, samples: 4−6) CF sputum. Supernatants (standardized amount: 30 μg protein/sample) were analyzed by Western blotting using a polyclonal anti-LL-37 antibody. Purified LL-37 was used as control (c). (B) Cleavage of endogenous LL-37 by CF sputum after incubation (0−6 h) in 100 mM acetate sodium, pH 5.5 containing 5 mM DTT and 0.01% Brij35 (buffer B) (a representative of the six samples is shown). Alternatively, supernatants were preincubated with E-64 (6 h). (C) Western blot of LL-37 degradation by human alveolar macrophages (AM). LL-37 (30 ng) was incubated for 0−24 h with AM in buffer B. In parallel, samples were incubated with E-64, CA-074, and Mu-Leu-Hph-VSPh prior to adding LL-37. Samples from CF sputum and alveolar macrophages were harvested in 100 mM sodium acetate, pH 5.0 (buffer A), containing a serine, asparatate, metallo, and cysteine peptidase inhibitor cocktail (0.5 mM PMSF, 0.5 mM EDTA, 40 μM pepstatin A, and 1 mM MMTS).

concentrations of LL-37 in CF samples ranged from 2 to 6 μg/mL. Its precursor hCAP18 (18 kDa) and immunoreactive forms of LL-37 with an apparent higher molecular weight, which may correspond to oligomeric forms, were also detected. A prolonged incubation time of CF samples (6 h) in the reaction buffer of cysteine cathepsins led to the complete degradation of LL-37 but not hCAP18 (Figure 1B). The hydrolysis was blocked by the broad-spectrum cathepsin inhibitor, E-64. Our previous work reported that elevated levels of active CatB and CatL were found in CF sputum in comparison to CatK and CatS, and that their concentrations did not depend on the degree of *P. aeruginosa* colonization.[33] Since alveolar macrophages in CF sputum are the major source of cathepsins, we evaluated their ability to degrade LL-37. Cell-free lysate from non-CF human alveolar macrophages readily degraded LL-37 after 24 h incubation, and the hydrolysis was impaired in the presence of E-64, CA-074 (a selective CatB inhibitor), and LHVS (a potent CatS inhibitor) (Figure 1C). Pro- and mature forms of CatB, K, L, and S were immunodetected in the lysate fraction (data not shown), and the active site concentrations of the cathepsins were determined by E-64 titration and estimated at 4.8 μM. In contrast, we did not detect significant hydrolysis of LL-37 upon incubation with the conditioned medium from the culture of macrophages buffered at pH 5.5, which contained lower concentrations of endopeptidase cysteine cathepsins (~200 nM). As previously reported,[39] the stability of LL-37 in CF sputum is likely due to the presence of anionic molecules including GAGs that interact with LL-37 and protect it from proteolysis. Taking these data into account, we investigated the individual contribution of CatB, K, L, and S to hydrolyze and inactivate LL-37 *in vitro* and the protective effects of GAGs.

CatK and CatS Degrade and Inactivate LL-37. LL-37 was incubated with increasing concentrations of purified CatB, L, K, and S (substrate/enzyme molar ratios = 1000 to 17600; as found in CF BALFs[11,39]) at pH 5.5 for 1 h at 37 °C, prior analysis of the degradation pattern of LL-37 by SDS-PAGE. CatS, CatK, and to a lesser extent CatB degraded LL-37 in a dose-dependent manner and generated truncated peptides with an apparent mass of ~2.3−2.8 kDa (Figure 2A). Release of smaller fragments was observed after prolonged incubation. Conversely, under similar conditions CatL did not cleave LL-37. Moreover, CatS, which is more efficient than CatK to cleave LL-37 at pH 5.5 (Figure 2B), hydrolyzed LL-37 at pH 7.4 (Figure 2C) and was more efficient than human neutrophil elastase (HNE) that is known to inactivate LL-37.[40] On the basis of findings that glycosaminoglycans (GAGs) inhibit LL-37 proteolysis,[39] LL-37 was incubated with chondroitin 4-sulfate (C4-S), heparin (HP), heparan sulfate (HS), and hyaluronic acid (HA) prior to adding CatK and CatS, respectively (Figure 2D,E). HP, HS, and C4-S, but not HA, inhibited in a dose-dependent manner the degradation of LL-37 by both proteases. To a lesser extent for HP, addition of NaCl restored the hydrolysis of LL-37 by both proteases in a dose-dependent manner (Figure 2F,G). In addition, digestion experiments of LL-37 with CatK and CatS were not impaired in the presence of 0.15 M NaCl. At neutral pH, LL-37 has a positive net charge of +6 (Table 1). The peptide carries 11 positive charges (6 lysine and 5 arginine residues) and 5 negative charges (3 glutamate and 2 aspartate residues). These results suggest that interactions between the negatively charged sulfated GAGs and LL-37 are mostly governed by electrostatic forces, which shield LL-37 from cathepsin-mediated degradation.

Next, cleavage products generated by CatB, K, L, and S were separated by RP-HPLC (Figure 3) and identified by MALDI-TOF mass spectrometry (Table 1). Three major hydrolysis products corresponding to cleavage sites Gln22-Arg23, Lys25-Asp26, and Arg29-Asn30 were detected after 30 min incubation with CatK (peaks 1, 6, and 7) (Figure 3A) and labeled as DF-19, DF-22, and NL-8 peptides, respectively. Prolonged incubation (4 h) led to the hydrolysis of both DF-19 and DF-22 peptides. Two additional LL-37 products were also detected and named RI-7 and KS-15. With the exception of an additional cleavage site (Arg7-Lys8), CatS showed the same cleavage specificity as CatK (Figure 3B). Compared to CatS and CatK, LL-37 was less sensitive to degradation by CatB

DOI: 10.1021/acs.biochem.5b00231
Biochemistry 2015, 54, 2785−2798

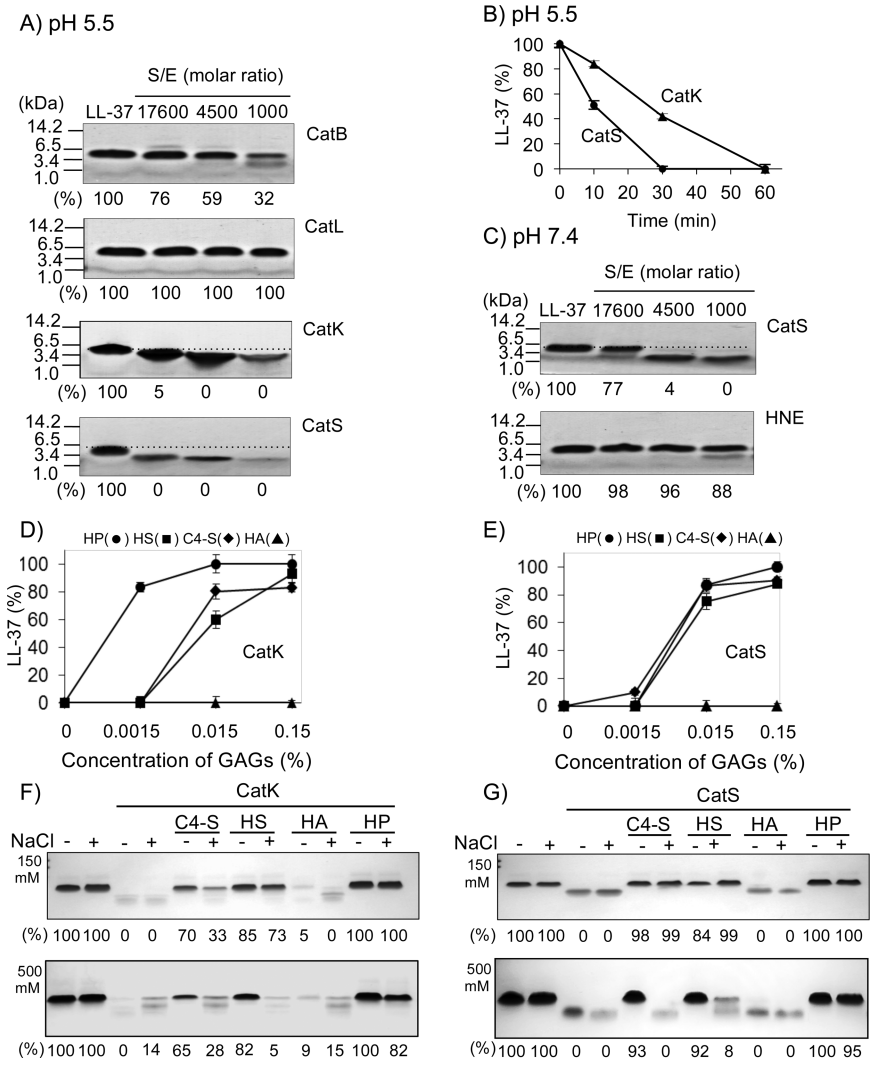

Figure 2. Hydrolysis of LL-37 by CatS and K and its protection by GAGs. (A) LL-37 (89 μM) was incubated in the presence or absence of CatB, K, L, and S (5 to 89 nM) in 100 mM sodium acetate buffer, pH 5.5, 2 mM DTT and 0.01% Brij35 for 1 h at 37 °C (buffer C). Incubation was made with three different S:E molar ratios. (B) Time dependence of LL-37 hydrolysis by CatS and CatK (S:E = 17,600). (C) LL-37 was incubated with CatS and HNE in their respective buffer (pH 7.4) for 1 h at 37 °C. Dashed line indicates the position of native LL-37. (D and E) Protection of LL-37 with glycosaminoglycans. LL-37 was incubated with CatK (D) and CatS (E) (S:E = 17 600) in the presence of increasing concentrations of heparin (HP), heparan sulfate (HS), chondroitin 4-sulfate (C4-S), and hyaluronic acid (HA) at pH 5.5 for 1 h. (F and G) The same experiment was performed in the presence of NaCl (150 and 500 mM). Samples were separated on a 8−25% SDS-PAGE under reducing conditions and gels were Coomassie stained with Brillant Blue G-250. The density of the remaining native LL-37 band was measured with ImageJ software (NIH software) and expressed as % of total LL-37 used (panels A, C, F, and G). Each experiment was performed at least two times.

(Figure 3C). We identified two cleavages occurring at the Arg19-Ile20 and Thr35-Glu36 bonds (Table 1). In contrast, CatL did not generate hydrolysis products (Figure 2A) and only after extended incubation times (4 h) a minor product was detected (peak 1, Figure 3D) corresponding to the DF-34 peptide. Cleavage occurred at the N-terminus at the Gly3-Asp4 bond (Table 1). As expected, the D-enantiomer of LL-37 (D-LL-37, i.e., each L-residue was replaced by a D-amino acid) was resistant to proteolysis by cathepsins under the same experimental conditions (data not shown).

Given the critical role of the midregion of LL-37 for the antimicrobial activity,[41] cleavage within this region would impair its biological activity. Therefore, Gram-negative (*P. aeruginosa* and *E. coli*) and Gram-positive bacteria (*S. aureus*) were tested for their antimicrobial susceptibility with increasing concentrations of LL-37 products. Radial diffusion assays indicated that both CatS and K, but not CatB and L, inactivated the antibacterial activity of LL-37 (S:E molar ratio = 4500) (Figure 4). However, when LL-37 was incubated with a high concentration of CatB (200 nM, i.e., molar ratio S:E = 1000) the antimicrobial activity of LL-37 products was partially impaired (data not shown). Conversely, when assays were performed with low concentration of CatS and CatK (10 nM, i.e., molar ratio S:E = 17 600), the antimicrobial activity of LL-37 products against Gram-negative bacteria was similar to that of the control LL-37 (data not shown). A moderate antimicrobial effect was observed against *S. aureus*. According to RP-HPLC analysis, LL-37 was completely degraded in the reaction mixtures, suggesting that among LL-37 products one has antimicrobial significance. To support this assumption, we focused on the DF-22 peptide for the following reasons: (i) DF-22 was generated by both CatS and CatK, (ii) it overlaps the central region of LL-37, and (iii) DF-22 was completely degraded after 4 h incubation with both enzymes (S:E molar

DOI: 10.1021/acs.biochem.5b00231
Biochemistry 2015, 54, 2785−2798

Table 1. Hydrolysis of LL-37 by Cats K, S, B, and L: Identification of the Cleavage Sites and Analysis of the LL-37 Products

Abbreviation	Mass[a] (Da)	Peak	Sequence	pI[b]	Net charge	GRAVY[c]	Agadir[c]
			K/S S K/S K/S K/S K/S K/S				
			1 10 20 30 37				
LL-37	4493.6	-	LLGDFFRKSKEKIGKEFKRIVQRIKDFLRNLVPRTES	10.6	+6	-0.724	5.10
			L B B				
CatK NL-8	915.5	1	NLVPRTES	6	+1	-0.825	0.00
KE-8	1047.6	2	KEFKRIVQ	10	+2	-0.975	0.04
DF-9	1118.7	3	DFFRKSKEK	9.7	+2	-2.044	0.07
KE-11	1444.8	4	KEFKRIVQRIK	11.1	+4	-1.064	0.19
DF-11	1354.7	5	DFFRKSKEKIG	9.7	+2	-1.300	0.14
DF-19	2383.3	6	DFFRKSKEKIGKEFKRIVQ	10.2	+4	-1.163	0.36
DF-22	2780.3	7	DFFRKSKEKIGKEFKRIVQRIK	10.6	+6	-1.182	0.74
CatS NL-8	915.5	1	NLVPRTES	6	+1	-0.825	0.00
KE-8	1047.6	2	KEFKRIVQ	10	+2	-0.975	0.04
DF-9	1118.7	3	DFFRKSKEK	9.7	+2	-2.044	0.07
RI-7	947.6	4	RIKDFLR	10.8	+2	-0.757	0.01
KE-11	1444.8	5	KEFKRIVQRIK	11.1	+4	-1.064	0.19
KS-15	1818.1	6	KSKEKIGKEFKRIVQ	10.2	+4	-1.313	0.25
DF-19	2383.3	7	DFFRKSKEKIGKEFKRIVQ	10.2	+4	-1.163	0.36
DF-22	2780.3	8	DFFRKSKEKIGKEFKRIVQRIK	10.6	+6	-1.182	0.74
CatB							
LL-19	2326.3	1	LLGDFFRKSKEKIGKEFKR	10.2	+4	-1.058	0.92
IV-16	1968.3	2	IVQRIKDFLRNLVPRT	11.7	+4	-0.150	1.46
CatL							
DF-34	4207.7	1	DFFRKSKEKIGKEFKRIVQRIKDFLRNLVPRTES	10.6	+6	-1.000	5.22

[a]Mass was determined by MALDI-TOF analysis. [b]pI was calculated with protparam (expasy.org/protparam). [c]Predictive algorithm (http://agadir.crg.es).

ratio = 4500). The peptide DF-22 was synthesized and tested for its antimicrobial activity (Table 2). Notably, the antimicrobial potency of DF-22 (MIC) was comparable to that of the full-length LL-37 ranging from 2 to 9 μM. This result was similar to a related LL-37 derived peptide, RK-19, which was reported to exhibit antimicrobial activity against *E. coli* and *S. aureus*.[42] Thus, deletion of the three N-terminal residues of DF-22, which yields RK-19, did not play a pivotal role in the antimicrobial activity against the bacterial strains tested. Moreover, a viability assay (Live/dead Baclight bacterial viability Kit) was performed with LL-37, DF-22, and RK-19. Nearly 50% of *P. aeruginosa* lost its viability following exposure to DF-22 or RK-19 with concentration of 1x the MIC for 3 h, whereas only 10% of *S. aureus* was killed following the same exposure with DF-22 and RK-19. In contrast, LL-37 killed 50% of both strains. Physicochemical properties of DF-22 (net charge, isoelectric point, and hydropathicity) compared to those of LL-37 (Table 1). Moreover, analysis of the helical wheel representation indicated that hydrophobic residues of DF-22 converged to one side and the hydrophilic residues to the other side of the helical axis as reported for LL-37 (Figure 5A). Conversely, we noted an important difference of the agadir score (helical content) between DF-22 (0.74) and LL-37 (5.1). Removal of 3 and 12 amino-acids from the N- and C-terminal domain, respectively, strongly decreased the propensity of LL-37 to form an α-helix. Accordingly, we did not observe an α-helical structure by CD spectra for DF-22 contrary to LL-37 (33% of α-helical content at pH 7.4 and 22% at pH 5.5) (Figure 5B). The low propensity of LL-37 to adopt an α-helical structure in phosphate buffer was reported previously.[43] CD spectra of RK-19 at both pH were comparable to that of LL-37 in water.[44] These results suggest that the antimicrobial activity of LL-37 does not primarily depend on the presence of an α-helix in solution.

Inhibition of CatL by LL-37. Recently, Pazgier et al. (2013)[17] reported that both LL-37 and hCAP18 caused an apparent inhibition of CatL activity at high concentrations (>1 μM). They suggested that the region involved in the inhibition is located within LL-37 and not in the N-terminal prodomain of hCAP18 (CLD), as proposed in a previous report.[13] To clarify this contradiction, we investigated in detail the mode of inhibition of CatL by LL-37. The Lineweaver−Burk double-reciprocal plots indicated that the inhibition of CatL is competitive and reversible, and Dixon plot analysis resulted in a K_i value of 150 nM (Figure 6A,B). Furthermore, the inhibition was stable within prolonged incubation times of 4 h. In contrast, both D-LL-37 enantiomer and scrambled Sc-LL-37 (same charge and net amino acid composition as native LL-37, without helical organization) did not inhibit CatL. While addition of NaCl restored the peptidase activity of CatL toward Z-Phe-Arg-AMC in a dose-dependent manner (Figure 6C), LL-37 still inhibited significantly CatL at physiologically relevant ionic strengths (0.1−0.5 M NaCl; $p < 0.05$). A K_i of 500 nM was determined in the presence of 0.15 M NaCl. Moreover, no hydrolysis of LL-37 was detected by SDS-PAGE analysis in the presence of CatL with increasing concentrations of NaCl (0.1−0.5 M, data not shown). This implies that electrostatic interactions are important for the binding of the positively charged LL-37 (pI = 10.6) to the negatively charged CatL (theoretical pI = 4.7) at pH 5.5. Preincubation of LL-37 with 15 to 150 μg/mL of C4-S, HP, or HS prevented the inhibition of CatL, while HA had no influence on the inhibition (data not shown).

On the other hand, no inhibition of CatK, S, and B was observed in the presence of LL-37, suggesting that critical residues located within the active site of CatL interact with LL-37. It is well established that the primary specificity site of cathepsins depends on S2−P2 interactions.[45] Comparison of the structures of CatL and CatK showed sequence differences

DOI: 10.1021/acs.biochem.5b00231
Biochemistry 2015, 54, 2785−2798

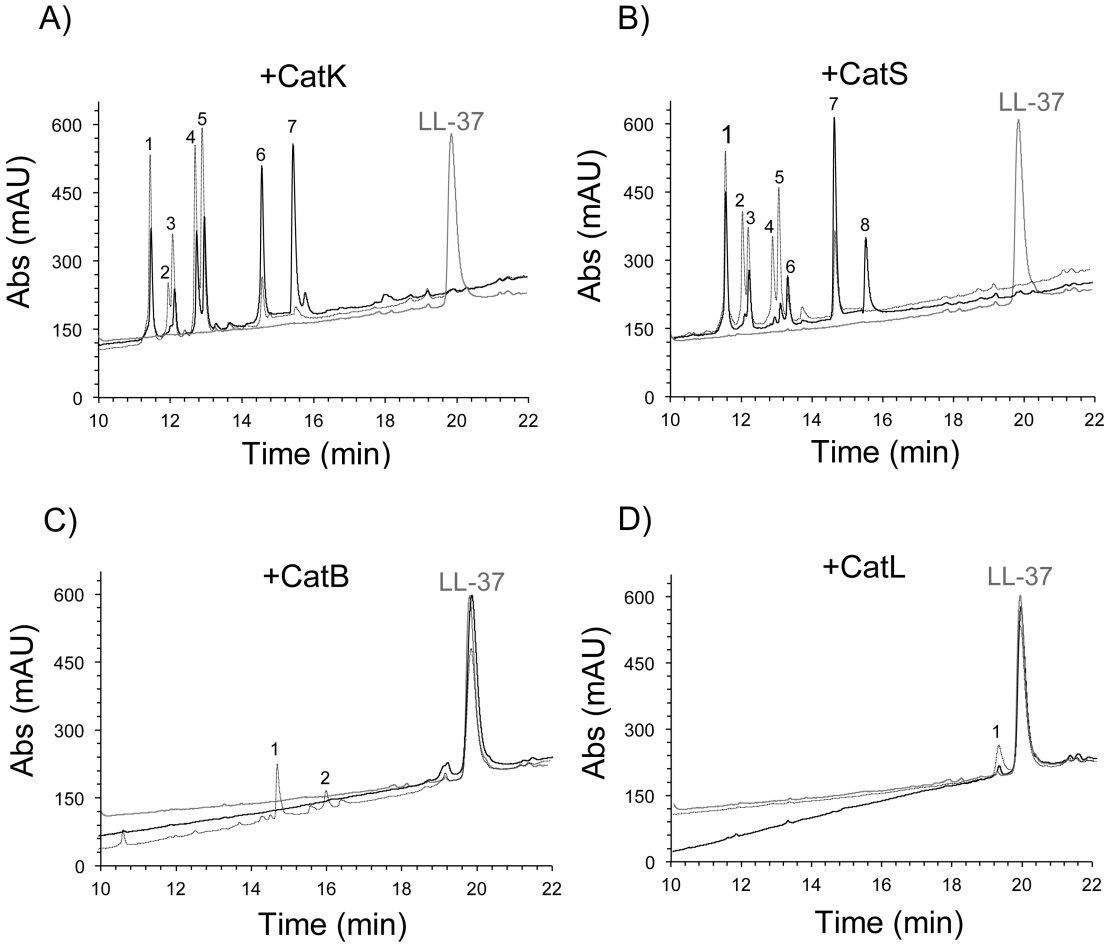

Figure 3. Analysis of LL-37 degradation products. LL-37 (89 μM) was incubated in the presence of CatK (panel A), CatS (panel B), CatB (panel C), and CatL (panel D) (S:E molar ratio = 4500) in buffer C for 30 min (full line) and 240 min (dotted line) at 37 °C. Control experiments used untreated LL-37 (light gray). Hydrolysis products were analyzed by RP-HPLC (C-18 column) as described in the Experimental Procedures. Chromatograms were recorded at 220 nm.

at residues 67 and 205 (papain numbering) in the S2 binding pocket, which form part of the wall and the bottom of this subsite, respectively.[46] The exchange of residues 67 and 205 of the S2 pocket of CatL (Leu67Tyr/Ala205Leu) by those present in CatK resulted in the complete hydrolysis of LL-37, as observed with the wild-type (wt) CatK (Figure 6D). Conversely, LL-37 hydrolysis was significantly decreased upon incubation with the S2 CatL-like CatK mutant (Tyr67Leu/Leu205Ala) (80% of remaining LL-37) compared to the complete degradation by wt CatK under the same conditions. Nevertheless, inhibition of the CatK variant presented a ~52-fold difference in K_i value (K_i = 7.8 μM) to that of wt CatL. These data indicate that the switch of the S2 subsite of CatK into a S2 CatL-like one was insufficient to fully mimic the inhibition of wt CatL by LL-37.

Subsequently, a library of synthetic truncated fragments obtained by sequential deletion of the N-terminus or C-terminus or from both ends of the full-length LL-37 was used to investigate their potentials to inhibit CatL as well as to identify the critical region interacting with the enzyme (Table 3). As the deletions progressed from the C-terminal end (LL-31, LL-25, LL-19, and LL-13), CatL activity was restored gradually. The removal of the first six amino acids from the N-terminal domain (RK-31) induced a ~2-fold loss of the inhibition compared to LL-37, while the removal of the next following N-terminal amino acids (IG-25, RI-19, and KD-13) completely abolished the inhibitory activity of LL-37. Deletion of six amino acids from both ends of native LL-37 (RK-25) resulted in a peptide which allowed about 80% of the CatL activity. Peptides containing the truncated central domain of LL-37 (IG-19, RK-19, IG-13) did not inhibit CatL. In addition, LL-37-truncated peptides were analyzed by RP-HPLC to evaluate their proteolytic resistance to CatL. After 1 h incubation period, peptides RK-25, RK-19, IG-25, IG-19, IG-13, RI-19, and KD-13 were almost completely degraded by CatL, whereas significant amounts (30−50%) of native peptides LL-31, LL-25, LL-19, LL-13, and RK-31 remained intact. With the exception of LL-37, LL-31, LL-25, LL-19, and LL-13 no significant correlation was measured between the inhibition of CatL and predicted α-helical content of truncated peptides (Table 3). These results indicated that the whole sequence of LL-37 is necessary for the inhibition of CatL.

Molecular Modeling of the Interactions between LL-37and CatL-. To provide insight into the mechanism of inhibition, molecular modeling studies were carried out to examine potential interaction sites of LL-37 with CatL. To achieve this, LL-37 was docked to the whole surface of CatL. Two clusters of docking solutions were obtained and featured LL-37 covering the active site of the enzyme in two different orientations (Figure 7A), which were referred to as forward

DOI: 10.1021/acs.biochem.5b00231
Biochemistry 2015, 54, 2785−2798

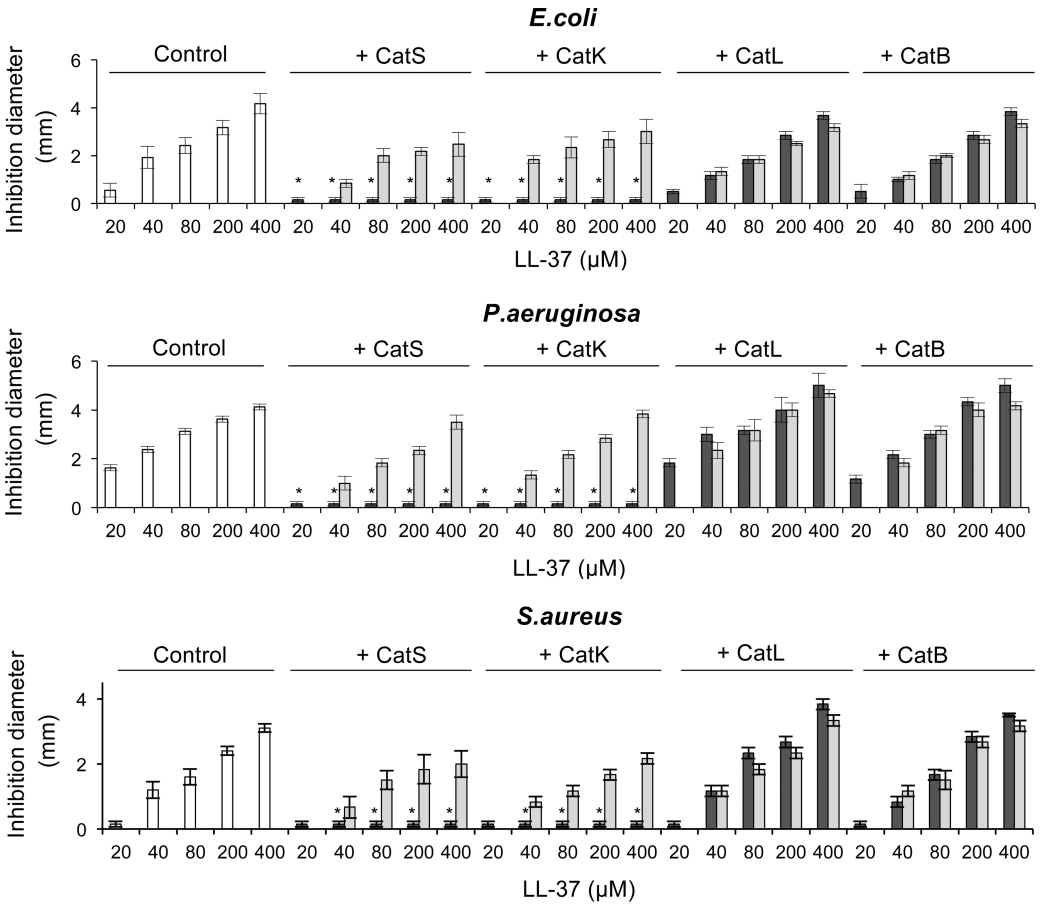

Figure 4. Inactivation of the antimicrobial activity of LL-37 by CatS and K. LL-37 (200 μM) was incubated either alone (white bar) or with Cats B, K, L, or S (44 nM) (dark gray) in buffer C for 6 h at 37 °C. Heat-inactivated enzymes were used as controls (light gray). After incubation, aliquots were taken from the reaction mixture and diluted 1:20, 1:10, 1:5, and 1:2. Samples were then precipitated to remove the enzyme and concentrated twice. Evaluation of antimicrobial activity against *E. coli*, *P. aeruginosa*, and *S. aureus* was assessed by radial diffusion assay method. Inhibition diameter of bacterial growth was measured and expressed in mm. Data are represented as mean ± SEM (n = 3). Statistical analysis was performed with the two way Mann−Whitney U test, and values were compared with the control (*: $p < 0.02$).

Table 2. Bacterial Minimal Inhibitory Concentration (MIC) of LL-37 and Synthetic Derived Fragments[a]

	MIC (μM)		
peptide	*P. aeruginosa*	*S. aureus*	*E. coli*
LL-37	2.7 ± 0.1	8.9 ± 2.7	7.6 ± 2.6
DF-22	2.2 ± 0.3	2.5 ± 0.2	3.3 ± 1.2
RK-19	2.4 ± 1.0	4.7 ± 1.0	3.2 ± 1.3

[a]MIC was assessed by radial diffusion assay. Results are expressed as mean ± SD (n = 3).

(i.e., the peptide is oriented in the way that it could be cleaved by the protease) and reverse orientations (the peptide is in the opposite orientation). The representative solutions from these two clusters were then simulated with molecular dynamics (MD), and free energies of binding were calculated (Table 4). MM-GBSA free energy calculations showed the crucial role of electrostatics for CatL/LL-37 interaction independently of the LL-37 orientation in the binding cleft. The catalytic domain of CatL, which is substantially more negatively charged than in other related cathepsins, favored interactions with positively charged LL-37. Although the total binding energy for LL-37 and CatK (ΔG_{total} = −80.3 ± 10 kcal/mol) was similar to that of CatL/LL-37, the electrostatic energy component for CatK (ΔG_{elect} = −221.6 ± 59 kcal/mol) was significantly less favorable (∼7-fold) as that of CatL. Predicted total binding energies for LL-37 and CatL were similar for both orientations suggesting that the reverse orientation is potentially accessible to the active site of CatL. To confirm this result, we tested *in vitro* a synthetic peptide (SE-37) corresponding to the reverse sequence of LL-37. Interestingly, SE-37, which adopts an α-helical structure at pH 7.4 but not at pH 5.5 (Figure 5B) inhibited CatL in the same range as LL-37 (K_i = 100 nM). Moreover, RP-HPLC analysis revealed no significant hydrolysis of SE-37 upon 30 min incubation with CatL, in contrast to that observed with CatB, K, and S. Next, the relative individual energy contributions of LL-37 residues to the binding with CatL were evaluated for LL-37 in both forward and reverse orientations (Figure 7B). Seventeen residues favored binding to CatL in both positions, while five negatively charged residues (Asp4, Glu11, Glu16, Asp26, and Glu36) as well as Gln22 and Ser37 had unfavorable contributions. It has to be noted that ΔG binding energies for Ile13, Lys15, Phe17, Lys18, Arg19, Ile20, and Val21 in the direct orientation were comparable to the data for the reverse orientation. Moreover, these residues covered the unprimed subsites (S1−S3) of CatL in both orientations. Noteworthy, analysis of binding free energy of native and LL-37 truncated peptides pointed out that there is a significant relationship between the binding energy and the apparent inhibition of CatL when the position of peptides are

DOI: 10.1021/acs.biochem.5b00231
Biochemistry 2015, 54, 2785−2798

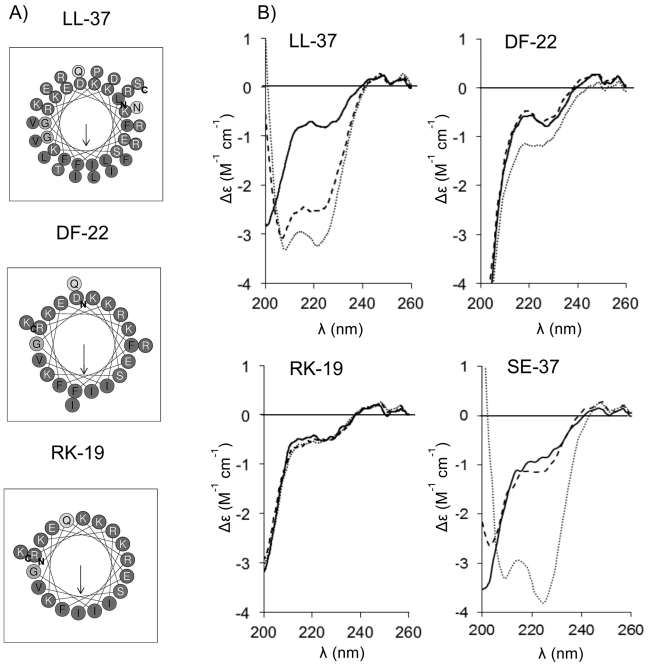

Figure 5. Secondary structure of LL-37 and its derivatives. (A) Helical wheel representation of LL-37, SE-37, DF-22, and RK-19 at pH 7.4 (http://heliquest.ipmc.cnrs.fr). The hydrophobic face is indicated with an arrow. Charged residues are mostly oriented to the opposite side. The N- and C-termini of each peptide are indicated. (B) CD spectra of LL-37, DF-22, RK-19, and SE-37 (20 μM) in water (full line) 100 mM phosphate sodium buffers (pH 5.5, dashed line, and 7.4, dotted line).

in the reverse orientation (Figure 7C). Pearson and Spearman correlation coefficients were 0.67 and 0.82, respectively. Peptides IG-19, IG-13, IG-25, RI-19, and KD-13, which did not inhibit CatL, exhibited a weaker binding energy compared to LL-37 truncated inhibitory peptides (LL-31, LL-25, LL-19, LL-13, RK-31, RK-25, and RK-19). Conversely, no significant correlation was measured when LL-37 truncated peptides were in the forward orientation.

DISCUSSION

As a key component of the innate immune system, the interest in LL-37 has been growing worldwide during the past decade. In CF, the innate immunity of the lungs is compromised, resulting to chronic infections by opportunistic pathogens (mainly *P. aeruginosa* and *S. aureus*). This defect is partially attributed to the inactivation of major AMPs including LL-37. A number of prior studies reported that cysteine cathepsins B, K, L, and S are expressed in human lung and their protein expression levels are increased during CF.[21,47] Moreover, several lines of evidence support that CatB, L, K, and S are involved in the proteolysis of structurally and functionally different AMPs such as lactoferrin, SLPI, SP-A, hBD-2 and -3.[21−24] However, we report here the presence of immunoreactive forms of LL-37 and its precursor hCAP-18 in the expectorations of CF patients. Subsequently these findings prompted us to investigate whether LL-37 is an inhibitor, a substrate, or combines both functions toward cathepsins. Previously, human cathelin-like domain (CLD), the N-terminal prodomain of hCAP-18, was described to inhibit at high concentration the peptidase activity of CatL.[13] In contrast, the CLD of porcine protegrin-3 enhanced CatL activity.[48] In both cases, authors suggested that CLD could interact with the active site of CatL, and putative conformational changes may occur, switching the CLD to act as an inhibitor or activator of CatL. Even though both human CLD and chicken cystatin share a common structural fold, the former lacks the three functional motifs of cystatins that are specifically involved in the inhibition of cysteine proteases (for review, see ref 48). Therefore, it could not be excluded that CLD might be a competitive substrate of CatL. Recently, it has been reported that human CLD was inactive against CatL, whereas both pro-cathelicidin and LL-37 impaired in a dose-dependent manner the CatL peptidase activity.[17] It has been suggested that LL-37 is likely the inhibitory domain of hCAP18/LL-37 against CatL. In light of these paradoxical reports, we decided first to characterize in detail the mode of inhibition of CatL by LL-37. We demonstrated that LL-37 is a selective and competitive CatL inhibitor, and that its positive charge and the sequence of LL-37 are critical for the inhibition of CatL. No apparent inhibition of the closely related Cats K, S, and B was measured in the presence of LL-37. In contrast, CatK, S, and to a lesser extent CatB degrade readily LL-37 *in vitro*, suggesting that singular residues located within the active site of CatL interact with LL-37. This selective interaction between CatL and LL-37 can be relinquished by altering two amino acids in the S2 pocket of the binding site of CatL (Leu67 and Ala205) into residues present in the CatK S2 subsite.[46] This double mutant (Leu67Tyr/Ala205Leu) became a potent LL-37-degrading CatL variant similar to CatK. In contrast, the (Tyr67Leu/Leu205Ala) CatK mutant lost most of its LL-37 degrading ability and was partially inhibited by this peptide. These findings underline the importance of residues Leu67 and Ala205 (papain numbering) for the interaction of LL-37 with CatL. Furthermore, as supported by *in vitro* and *in silico* experiments, LL-37 may adopt two directions in the active site of CatL (i.e., in a forward or in a reverse direction to the conventional substrate binding cleft). This latter arrangement may confer an inhibitory capacity of LL-37 against CatL as previously observed for the propeptide of CatL that covers the substrate-binding site of CatL in an opposite direction to that of the bound substrate.[49] To our knowledge, CatL is the only human cysteine cathepsin identified to date that is inhibited by LL-37. This may contribute in part to the presence of LL-37 in CF sputum despite the presence of elevated concentrations of active CatL, which is the most abundant cysteine endopeptidase with CatB in comparison to CatS and CatK.[33] While the current study characterized the mode of inhibition, the impact of the inhibitory capacity of LL-37 *in vivo* remains unclear, in particular, whether LL-37 affects the proteolytic activity of CatL in the ECM, and further studies are clearly warranted.

On the other hand, we found that cysteine cathepsins from treated non-CF human alveolar macrophages readily cleaved LL-37, suggesting the role of cathepsins in the degradation of LL-37 *in vivo*. We identified that, among the cysteine endopeptidases expressed by alveolar macrophages, CatK and S are the most effective cathepsins to degrade LL-37 *in vitro*. As a result, both CatK and S abolished the antimicrobial activity of LL-37 against *P. aeruginosa*, *E. coli*, and *S. aureus*. Alternatively, submitting macrophages lysates to CA-074, a selective inhibitor of CatB, reduced the degradation of LL-37. The housekeeping CatB activity accounted for ∼50% (e.g., ∼2.4 μM) of the total cathepsin endopeptidase activities in macrophages lysates (data not shown). This suggests that a high concentration of CatB is probably required to cleave LL-37, in agreement with our experimental assays. Therefore, cysteine cathepsins participate

DOI: 10.1021/acs.biochem.5b00231
Biochemistry 2015, 54, 2785−2798

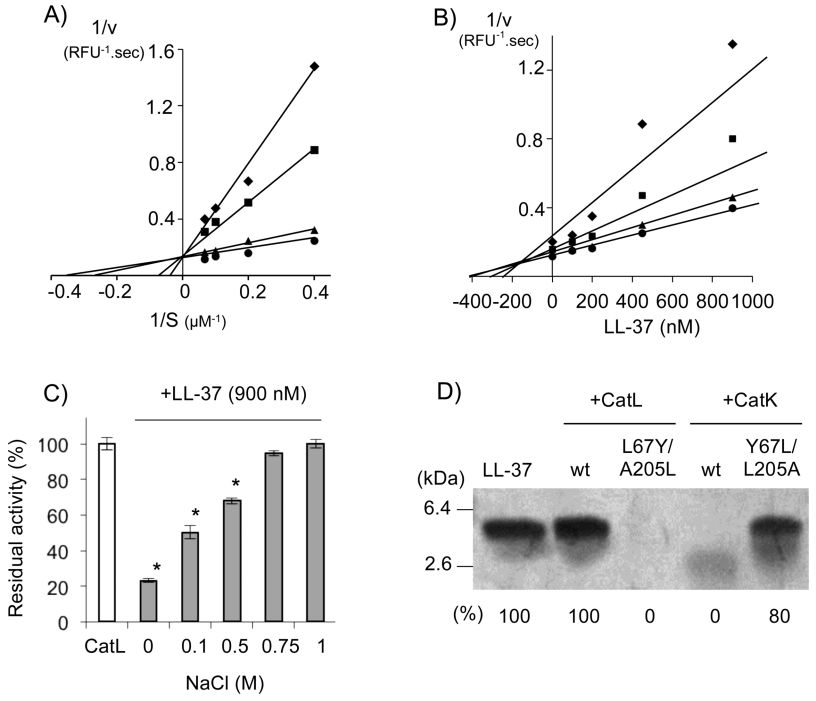

Figure 6. Inhibition of CatL by LL-37. (A) CatL (2 nM) was incubated either alone (filled circle) or with LL-37 (900 nM: filled diamond, 450 nM: filled square and 200 nM: filled triangle) in 100 mM sodium acetate buffer, pH 5.5, 2 mM DTT, and 0.01% Brij35. Residual activity was measured toward the fluorogenic substrate (S) Z-Phe-Arg-AMC (2.5−20 μM). Determination of type of inhibition was performed using the Lineweaver−Burk plot. The velocity (v) is expressed as relative fluorescence emission units (RFU) per second. (B) Dixon plot representation. CatL (2 nM) was incubated with increasing concentrations of LL-37, and residual activity was monitored against different concentrations of Z-Phe-Arg-AMC (2.5 μM: filled diamond, 5 μM: filled square, 10 μM: filled triangle, 15 μM: filled circle). (C) Residual activity of CatL (2 nM) in the presence of LL-37 (900 nM) and increasing concentrations of NaCl (0.1−1 M). Assays were performed in triplicate (n = 2). Residual activity is expressed as percentage of the corresponding control. Statistical analysis was performed with a two-way Mann and Whitney U test (*: $p < 0.02$). (D) LL-37 (89 μM) was incubated with CatL, K, and their respective S2 mutant (20 nM) for 1 h at 37 °C. Samples were separated on a 8−25% SDS-PAGE under reducing conditions, and gels were Coomassie stained with Brilliant Blue G-250.

Table 3. Inhibition of CatL by LL-37 Truncated Peptide Library[a]

Peptide	Sequence	AGADIR	Inhibition (%) (mean ± SD)
LL-37	LLGDFFRKSKEKIGKEFKRIVQRIKDFLRNLVPRTES	5.10	74.5 ± 1 *
LL-31	LLGDFFRKSKEKIGKEFKRIVQRIKDFLRNL	3.72	66.5 ± 1 *
LL-25	LLGDFFRKSKEKIGKEFKRIVQRIK	1.19	48.8 ± 2 *
LL-19	LLGDFFRKSKEKIGKEFKR	0.92	27.2 ± 6 *
LL-13	LLGDFFRKSKEKI	0.84	15.5 ± 2 *
RK-25	RKSKEKIGKEFKRIVQRIKDFLRNL	4.06	18.7 ± 2 *
IG-19	IGKEFKRIVQRIKDFLRNL	4.33	0.9 ± 2
RK-19	RKSKEKIGKEFKRIVQRIK	0.73	10.3 ± 7 *
IG-13	IGKEFKRIVQRIK	0.71	0
RK-31	RKSKEKIGKEFKRIVQRIKDFLRNLVPRTES	5.68	35.6 ± 5 *
IG-25	IGKEFKRIVQRIKDFLRNLVPRTES	5.87	0
RI-19	RIVQRIKDFLRNLVPRTES	2.08	0
KD-13	KDFLRNLVPRTES	0.09	0

[a]Residual activity of CatL (2 nM) toward Z-Phe-Arg-MCA (20 μM) in the presence of LL-37 truncated peptides (900 nM). Assays were performed in triplicate (n = 2) (*, $p < 0.02$).

in concert with other identified proteases in the degradation of numerous key innate immunity peptides/proteins, including LL-37, and thus may display immunomodulatory activities during CF.[50] Nevertheless, the degree to which AMPs are cleaved and inactivated by cysteine cathepsins during CF may depend on cellular components present in the altered pulmonary milieu. Intriguingly, contrary to LL-37, defensin hBD-2 and surfactant protein SP-A were extensively degraded

DOI: 10.1021/acs.biochem.5b00231
Biochemistry 2015, 54, 2785−2798

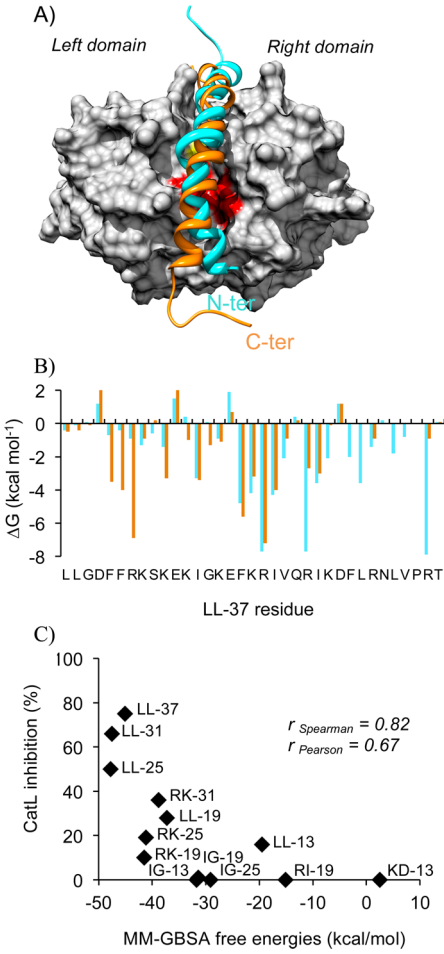

Figure 7. Molecular modeling of LL-37 recognition by CatL. (A) Molecular docking of LL-37 in the forward (blue helix) and reverse orientation (orange helix) into the active site cleft of CatL (gray surface). The residues of the S2 pocket of CatL are highlighted as a red surface and residue Cys25 of the active site in yellow. (B) MM-GBSA per residue free energy decomposition for LL-37 in the forward (blue bar) and the reverse (orange bar) orientations. (C) MM-GBSA free energies for truncated LL-37 peptides in the reverse orientation are plotted against the inhibition of CatL. The significance of the correlation between MM-GBSA free energies and inhibition was assessed with Spearman and Pearson coefficients.

Table 4. MM-GBSA Binding Free Energy (kcal/mol) of LL-37 with CatL

	ΔG_{total}	ΔG_{elect}	ΔG_{vdw}
LL-37			
forward position	−81.1 ± 7.7	−1650.9 ± 72.4	−92.4 ± 9.2
reverse position	−73.4 ± 7.5	−1594.5 ± 66.1	−83.4 ± 9.0

in both Ps+ and Ps− CF samples tested (data not shown). Moreover hBD-2 is susceptible to degradation and inactivation by cysteine cathepsins B, L, and S,[21] while SP-A is degraded specifically by CatS *in vitro*.[24] One plausible explanation of the presence of intact LL-37 is the binding of LL-37 to anionic molecules (e.g., DNA, F-actin, and GAGs) may protect it from proteolysis by CatS and CatK in CF sputum, as it has been previously reported for different host proteases including serine and acidic proteases (HNE, proteinase 3, and CatD)[39] as well as proteases released from *P. aeruginosa* and *S. aureus*.[51,52] McElvaney and colleagues reported that high sodium concentration is required to liberate LL-37 in CF bronchoalveolar lavage suggesting that LL-37 binds tightly to GAGs, likely due to electrostatic interactions.[39] Consistently, we report that high concentrations (0.15%) of sulfated GAGs (C4-S, HS, and HP) protect LL-37 from proteolysis by CatK and S similarly to that observed for other proteases.[39,51−54] A consensus heparin-binding cardin motif XBBXBX (where X represents hydrophobic or uncharged residue, and B represents a basic residue) is found at the N-terminal part of LL-37 between Phe6 and Glu11. This site was sensitive to cleavage by CatK and S. Protection of LL-37 by sulfated GAGs (0.15%) was partially impaired by 150 mM NaCl and fully abolished at higher concentrations (500 mM), except for HP, which is the most sulfated GAG with an average of ∼2.5 sulfate groups/disaccharide, while C4-S and HS have ∼0.9 sulfate group/disaccharide. Moreover, we previously characterized that CatS peptidase activity was inhibited by C4-S and HS in a dose-dependent manner,[55] which mounted up in the resistance of LL-37 to proteolysis.

It would be interesting to determine whether cysteine cathepsins operate similarly in skin and other sites where LL-37 is found. It was proposed that host proteases, including CatK, elastase, CatG, and MMP-9, present in the gingival crevicular fluid from periodontitis patients, may contribute in concert with bacterial proteases to the degradation of LL-37.[56] Furthermore, since LL-37 is expressed in different tissues either constitutively or induced during inflammation, it cannot be ruled out that the hydrolysis of LL-37, which is cytotoxic to eukaryotic cells at a high concentration, by cysteine cathepsins is beneficial.[44,57,58] Taken together with other studies, we provide further indication that cysteine cathepsins are new biologically relevant players in the process of degradation and inactivation of major AMPs including, SLPI, lactoferrin, SP-A, and LL-37. More broadly, the importance of regulating the activity of cathepsins for control of antimicrobial activity in lungs may be critical in the pathophysiology of CF.

AUTHOR INFORMATION

Corresponding Author

*Address: INSERM, UMR 1100 "Pathologies Pulmonaires: Protéolyse et Aérosolthérapie"/CEPR, Université François Rabelais, Faculté de Médecine, 10 Boulevard Tonnellé, F-37032 Tours cedex, France. Tel: (+33) 24736604. E-mail: fabien.lecaille@univ-tours.fr.

Funding

We acknowledge the Institut National de la Santé et de la Recherche Médicale (INSERM) for institutional funding. P.M.A. holds a doctoral fellowship from INSERM and the Région Centre, France. M.T.P. group is funded by the German Research Council (SFB-TRR67; A7). K.N. and J.G.M.B. were supported by a grant from the University of Amsterdam for research into the focal point Oral Infections and Inflammation.

Notes

The authors declare no competing financial interest.

ACKNOWLEDGMENTS

We kindly thank Dr. Sylvain Marchand-Adam (Inserm UMR 1100, Service de Pneumologie, CHRU de Tours, France) for providing human BALF and Dr. Patrick Plésiat (Laboratoire de Bactériologie, CHU Saint Jean Minjoz, Besançon, France) for CF sputum samples. We thank Dr. Ahlame Saidi (Inserm UMR 1100, Tours, France) for her technical assistance. Mu-Leu-Hph-

DOI: 10.1021/acs.biochem.5b00231
Biochemistry 2015, 54, 2785−2798

VSPh was kindly provided by Dr. J. H. McKerrow (Skaggs School of Pharmacy and Pharmaceutical Sciences, University of California San Diego, La Jolla, CA, USA).

■ ABBREVIATIONS

AEBSF, 4-(2-aminoethyl) benzenesulfonyl fluoride hydrochloride; BALF, bronchoalveolar lavage fluid; Cat, cysteine cathepsin; CA-074, *N*-(L-3-trans-propylcarbamoyloxirane-2-carbonyl)-L-isoleucyl-L-proline; CD, circular dichroism; CF, cystic fibrosis; CLD, cathelin-like domain; DTT, dithiothreitol; E-64, L-3-carboxy-*trans*-2,3-epoxy-propionyl-leucylamide-(4-guanido)-butane; ECM, extracellular matrix; GAGs, glycosaminoglycans; HAM, human alveolar macrophage; hBD, human beta-defensin; hCAP, human cathelicidin antimicrobial peptide; HNE, human neutrophil elastase; LHVS, morpholinourea-leucinyl-homophenylalanine-vinyl-sulfone; MIC, minimal inhibitory concentration; MD, molecular dynamic; MM-GBSA, molecular mechanics-generalized Born surface area; MMTS, *S*-methyl thiomethanesulfonate; PMSF, phenylmethylsulfonyl fluoride; proCat, procathepsin; SP-A, surfactant protein A

■ REFERENCES

(1) Hiemstra, P. S. (2007) The role of epithelial beta-defensins and cathelicidins in host defense of the lung. *Exp. Lung Res. 33*, 537−542.
(2) Gallo, R. L., and Nizet, V. (2003) Endogenous production of antimicrobial peptides in innate immunity and human disease. *Curr. Allergy Asthma Rep. 3*, 402−409.
(3) Smith, J. J., Travis, S. M., Greenberg, E. P., and Welsh, M. J. (1996) Cystic Fibrosis Airway Epithelia Fail to Kill Bacteria Because of Abnormal Airway Surface Fluid. *Cell 85*, 229−236.
(4) Bals, R., Weiner, D. J., Meegalla, R. L., Accurso, F., and Wilson, J. M. (2001) Salt-Independent Abnormality of Antimicrobial Activity in Cystic Fibrosis Airway Surface Fluid. *Am. J. Respir. Cell Mol. Biol. 25*, 21−25.
(5) Goldman, M. J., Anderson, G. M., Stolzenberg, E. D., Kari, U. P., Zasloff, M., and Wilson, J. M. (1997) Human *β*-Defensin-1 Is a Salt-Sensitive Antibiotic in Lung That Is Inactivated in Cystic Fibrosis. *Cell 88*, 553−560.
(6) Weiner, D. J., Bucki, R., and Janmey, P. A. (2003) The Antimicrobial Activity of the Cathelicidin LL37 Is Inhibited by F-actin Bundles and Restored by Gelsolin. *Am. J. Respir. Cell Mol. Biol. 28*, 738−745.
(7) Bucki, R., Byfield, F. J., and Janmey, P. A. (2007) Release of the antimicrobial peptide LL-37 from DNA/F-actin bundles in cystic fibrosis sputum. *Eur. Respir. J. 29*, 624−632.
(8) Herasimenka, Y., Benincasa, M., Mattiuzzo, M., Cescutti, P., Gennaro, R., and Rizzo, R. (2005) Interaction of antimicrobial peptides with bacterial polysaccharides from lung pathogens. *Peptides 26*, 1127−1132.
(9) Benincasa, M., Mattiuzzo, M., Herasimenka, Y., Cescutti, P., Rizzo, R., and Gennaro, R. (2009) Activity of antimicrobial peptides in the presence of polysaccharides produced by pulmonary pathogens. *J. Pept. Sci. 15*, 595−600.
(10) Bucki, R., Namiot, D. B., Namiot, Z., Savage, P. B., and Janmey, P. A. (2008) Salivary mucins inhibit antibacterial activity of the cathelicidin-derived LL-37 peptide but not the cationic steroid CSA-13. *J. Antimicrob. Chemother. 62*, 329−335.
(11) Chen, C. I.-U., Schaller-Bals, S., Paul, K. P., Wahn, U., and Bals, R. (2004) *β*-defensins and LL-37 in bronchoalveolar lavage fluid of patients with cystic fibrosis. *J. Cystic Fibrosis 3*, 45−50.
(12) Xiao, W., Hsu, Y.-P., Ishizaka, A., Kirikae, T., and Moss, R. B. (2005) Sputum cathelicidin, urokinase plasminogen activation system components, and cytokines discriminate cystic fibrosis, COPD, and asthma inflammation. *Chest 128*, 2316−2326.
(13) Zaiou, M., Nizet, V., and Gallo, R. L. (2003) Antimicrobial and Protease Inhibitory Functions of the Human Cathelicidin (hCAP18/LL-37) Prosequence. *J. Investig. Dermatol. 120*, 810−816.
(14) Morizane, S., Yamasaki, K., Kabigting, F. D., and Gallo, R. L. (2010) Kallikrein expression and cathelicidin processing are independently controlled in keratinocytes by calcium, vitamin D(3), and retinoic acid. *J. Invest. Dermatol. 130*, 1297−1306.
(15) Sørensen, O. E., Follin, P., Johnsen, A. H., Calafat, J., Tjabringa, G. S., Hiemstra, P. S., and Borregaard, N. (2001) Human cathelicidin, hCAP-18, is processed to the antimicrobial peptide LL-37 by extracellular cleavage with proteinase 3. *Blood 97*, 3951−3959.
(16) Eick, S., Puklo, M., Adamowicz, K., Kantyka, T., Hiemstra, P., Stennicke, H., Guentsch, A., Schacher, B., Eickholz, P., and Potempa, J. (2014) Lack of cathelicidin processing in Papillon-Lefèvre syndrome patients reveals essential role of LL-37 in periodontal homeostasis. *Orphanet. J. Rare Dis. 9*, 148.
(17) Pazgier, M., Ericksen, B., Ling, M., Toth, E., Shi, J., Li, X., Galliher-Beckley, A., Lan, L., Zou, G., Zhan, C., Yuan, W., Pozharski, E., and Lu, W. (2013) Structural and functional analysis of the pro-domain of human cathelicidin, LL-37. *Biochemistry 52*, 1547−1558.
(18) Lee, C.-C., Sun, Y., Qian, S., and Huang, H. W. (2011) Transmembrane Pores Formed by Human Antimicrobial Peptide LL-37. *Biophys. J. 100*, 1688−1696.
(19) Scott, M. G., Davidson, D. J., Gold, M. R., Bowdish, D., and Hancock, R. E. W. (2002) The Human Antimicrobial Peptide LL-37 Is a Multifunctional Modulator of Innate Immune Responses. *J. Immunol. 169*, 3883−3891.
(20) Linde, A., Lushington, G. H., Abello, J., and Melgarejo, T. (2013) Clinical Relevance of Cathelicidin in Infectious Disease. *J. Clin. Cell. Immunol. S-13*, 003.
(21) Taggart, C. C., Greene, C. M., Smith, S. G., Levine, R. L., McCray, P. B., Jr., O'Neill, S., and McElvaney, N. G. (2003) Inactivation of human beta-defensins 2 and 3 by elastolytic cathepsins. *J. Immunol. 171*, 931−937.
(22) Taggart, C. C., Lowe, G. J., Greene, C. M., Mulgrew, A. T., O'Neill, S. J., Levine, R. L., and McElvaney, N. G. (2001) Cathepsin B, L, and S cleave and inactivate secretory leucoprotease inhibitor. *J. Biol. Chem. 276*, 33345−33352.
(23) Rogan, M. P., Taggart, C. C., Greene, C. M., Murphy, P. G., O'Neill, S. J., and McElvaney, N. G. (2004) Loss of microbicidal activity and increased formation of biofilm due to decreased lactoferrin activity in patients with cystic fibrosis. *J. Infect. Dis. 190*, 1245−1253.
(24) Lecaille, F., Naudin, C., Sage, J., Joulin-Giet, A., Courty, A., Andrault, P.-M., Veldhuizen, R. A. W., Possmayer, F., and Lalmanach, G. (2013) Specific cleavage of the lung surfactant protein A by human cathepsin S may impair its antibacterial properties. *Int. J. Biochem. Cell Biol. 45*, 1701−1709.
(25) Veillard, F., Lecaille, F., and Lalmanach, G. (2008) Lung cysteine cathepsins: intruders or unorthodox contributors to the kallikrein-kinin system? *Int. J. Biochem. Cell Biol. 40*, 1079−1094.
(26) Fonović, M., and Turk, B. (2014) Cysteine cathepsins and extracellular matrix degradation. *Biochim. Biophys. Acta 1840*, 2560−2570.
(27) Lalmanach, G., Saidi, A., Marchand-Adam, S., Lecaille, F., and Kasabova, M. (2015) Cysteine cathepsins and cystatins: from ancillary tasks to prominent status in lung diseases. *Biol. Chem. 396*, 111−130.
(28) Lecaille, F., Vandier, C., Godat, E., Hervé-Grépinet, V., Brömme, D., and Lalmanach, G. (2007) Modulation of hypotensive effects of kinins by cathepsin K. *Arch. Biochem. Biophys. 459*, 129−136.
(29) Serveau, C., Moreau, T., Zhou, G. X., ElMoujahed, A., Chao, J., and Gauthier, F. (1992) Inhibition of rat tissue kallikrein gene family members by rat kallikrein-binding protein and alpha 1-proteinase inhibitor. *FEBS Lett. 309*, 405−408.
(30) Den Hertog, A. L., van Marle, J., Veerman, E. C. I., Valentijn-Benz, M., Nazmi, K., Kalay, H., Grün, C. H., Van't Hof, W., Bolscher, J. G. M., and Nieuw Amerongen, A. V. (2006) The human cathelicidin peptide LL-37 and truncated variants induce segregation of lipids and proteins in the plasma membrane of Candida albicans. *Biol. Chem. 387*, 1495−1502.
(31) Godat, E., Chowdhury, S., Lecaille, F., Belghazi, M., Purisima, E. O., and Lalmanach, G. (2005) Inhibition of a cathepsin L-like cysteine

DOI: 10.1021/acs.biochem.5b00231
Biochemistry 2015, 54, 2785−2798

protease by a chimeric propeptide-derived inhibitor. *Biochemistry 44*, 10486−10493.
(32) Kasabova, M., Joulin-Giet, A., Lecaille, F., Saidi, A., Marchand-Adam, S., and Lalmanach, G. (2014) Human cystatin C: a new biomarker of idiopathic pulmonary fibrosis? *Proteomics Clin. Appl. 8*, 447−453.
(33) Naudin, C., Joulin-Giet, A., Couetdic, G., Plésiat, P., Szymanska, A., Gorna, E., Gauthier, F., Kasprzykowski, F., Lecaille, F., and Lalmanach, G. (2011) Human Cysteine Cathepsins Are Not Reliable Markers of Infection by Pseudomonas aeruginosa in Cystic Fibrosis. *PLoS One 6*, e25577.
(34) Lehrer, R. I., Rosenman, M., Harwig, S. S. S. L., Jackson, R., and Eisenhauer, P. (1991) Ultrasensitive assays for endogenous antimicrobial polypeptides. *J. Immunol. Methods 137*, 167−173.
(35) Kyte, J., and Doolittle, R. F. (1982) A simple method for displaying the hydropathic character of a protein. *J. Mol. Biol. 157*, 105−132.
(36) Comeau, S. R., Gatchell, D. W., Vajda, S., and Camacho, C. J. (2004) ClusPro: a fully automated algorithm for protein-protein docking. *Nucleic Acids Res. 32*, W96−99.
(37) Case, D. A., Darden, T. A., Cheatham, T. E., Simmerling, C. L., Wang, J., Duke, R. E., Luo, R., Walker, R. C., Zhang, W., Merz, K. M., Wang, B., Hayik, S., Roitberg, A., Seabra, G., Kolossvary, I., Wong, K. F., Paesani, F., Vanicek, J., Liu, J., Wu, X., Brozell, S. R., Steinbrecher, T., Gohlke, H., Cai, Q., Ye, X., Wang, J., Hsieh, M.-J., Hornak, V., Cui, G., Roe, D. R., Mathews, D. H., Seetin, M. G., Sagui, C., Babin, V., Luchko, T., Gusarov, S., Kovalenko, A., Kollman, P. A., and Roberts, B. P. (2010) Amber 11, University of California. Available from: http://infoscience.epfl.ch/record/150146.
(38) R Team (2006) *R Lang. Environ. Stat. Comput.*, http://www.R-project.org.
(39) Bergsson, G., Reeves, E. P., McNally, P., Chotirmall, S. H., Greene, C. M., Greally, P., Murphy, P., O'Neill, S. J., and McElvaney, N. G. (2009) LL-37 Complexation with Glycosaminoglycans in Cystic Fibrosis Lungs Inhibits Antimicrobial Activity, Which Can Be Restored by Hypertonic Saline. *J. Immunol. 183*, 543−551.
(40) Strömstedt, A. A., Pasupuleti, M., Schmidtchen, A., and Malmsten, M. (2009) Evaluation of Strategies for Improving Proteolytic Resistance of Antimicrobial Peptides by Using Variants of EFK17, an Internal Segment of LL-37. *Antimicrob. Agents Chemother. 53*, 593−602.
(41) Vandamme, D., Landuyt, B., Luyten, W., and Schoofs, L. (2012) A comprehensive summary of LL-37, the factotum human cathelicidin peptide. *Cell. Immunol. 280*, 22−35.
(42) Braff, M. H., Hawkins, M. A., Di Nardo, A., Lopez-Garcia, B., Howell, M. D., Wong, C., Lin, K., Streib, J. E., Dorschner, R., Leung, D. Y. M., and Gallo, R. L. (2005) Structure-function relationships among human cathelicidin peptides: dissociation of antimicrobial properties from host immunostimulatory activities. *J. Immunol. 174*, 4271−4278.
(43) Molhoek, E. M., den Hertog, A. L., de Vries, A.-M. B. C., Nazmi, K., Veerman, E. C. I., Hartgers, F. C., Yazdanbakhsh, M., Bikker, F. J., and van der Kleij, D. (2009) Structure-function relationship of the human antimicrobial peptide LL-37 and LL-37 fragments in the modulation of TLR responses. *Biol. Chem. 390*, 295−303.
(44) Johansson, J., Gudmundsson, G. H., Rottenberg, M. E., Berndt, K. D., and Agerberth, B. (1998) Conformation-dependent antibacterial activity of the naturally occurring human peptide LL-37. *J. Biol. Chem. 273*, 3718−3724.
(45) Choe, Y., Leonetti, F., Greenbaum, D. C., Lecaille, F., Bogyo, M., Brömme, D., Ellman, J. A., and Craik, C. S. (2006) Substrate profiling of cysteine proteases using a combinatorial peptide library identifies functionally unique specificities. *J. Biol. Chem. 281*, 12824−12832.
(46) Lecaille, F., Chowdhury, S., Purisima, E., Brömme, D., and Lalmanach, G. (2007) The S2 subsites of cathepsins K and L and their contribution to collagen degradation. *Protein Sci. 16*, 662−670.
(47) Weldon, S., McNally, P., McAuley, D. F., Oglesby, I. K., Wohlford-Lenane, C. L., Bartlett, J. A., Scott, C. J., McElvaney, N. G., Greene, C. M., McCray, P. B., and Taggart, C. C. (2014) miR-31 dysregulation in cystic fibrosis airways contributes to increased pulmonary cathepsin S production. *Am. J. Respir. Crit. Care Med. 190*, 165−174.
(48) Zhu, S., Wei, L., Yamasaki, K., and Gallo, R. L. (2008) Activation of cathepsin L by the cathelin-like domain of protegrin-3. *Mol. Immunol. 45*, 2531−2536.
(49) Coulombe, R., Grochulski, P., Sivaraman, J., Ménard, R., Mort, J. S., and Cygler, M. (1996) Structure of human procathepsin L reveals the molecular basis of inhibition by the prosegment. *EMBO J. 15*, 5492−5503.
(50) Kasabova, M., Saidi, A., Naudin, C., Sage, J., Lecaille, F., and Lalmanach, G. (2011) Cysteine Cathepsins: Markers and Therapy Targets in Lung Disorders. *Clin. Rev. Bone Miner. Metab 9*, 148−161.
(51) Schmidtchen, A., Frick, I.-M., Andersson, E., Tapper, H., and Björck, L. (2002) Proteinases of common pathogenic bacteria degrade and inactivate the antibacterial peptide LL-37. *Mol. Microbiol. 46*, 157−168.
(52) Sieprawska-Lupa, M., Mydel, P., Krawczyk, K., Wójcik, K., Puklo, M., Lupa, B., Suder, P., Silberring, J., Reed, M., Pohl, J., Shafer, W., McAleese, F., Foster, T., Travis, J., and Potempa, J. (2004) Degradation of Human Antimicrobial Peptide LL-37 by Staphylococcus aureus-Derived Proteinases. *Antimicrob. Agents Chemother. 48*, 4673−4679.
(53) Koziel, J., Karim, A. Y., Przybyszewska, K., Ksiazek, M., Rapala-Kozik, M., Nguyen, K.-A., and Potempa, J. (2010) Proteolytic inactivation of LL-37 by karilysin, a novel virulence mechanism of Tannerella forsythia. *J. Innate Immun. 2*, 288−293.
(54) Belas, R., Manos, J., and Suvanasuthi, R. (2004) Proteus mirabilis ZapA metalloprotease degrades a broad spectrum of substrates, including antimicrobial peptides. *Infect. Immun. 72*, 5159−5167.
(55) Sage, J., Mallèvre, F., Barbarin-Costes, F., Samsonov, S. A., Gehrcke, J.-P., Pisabarro, M. T., Perrier, E., Schnebert, S., Roget, A., Livache, T., Nizard, C., Lalmanach, G., and Lecaille, F. (2013) Binding of Chondroitin 4-Sulfate to Cathepsin S Regulates Its Enzymatic Activity. *Biochemistry 52*, 6487−6498.
(56) McCrudden, M. T. C., Orr, D. F., Yu, Y., Coulter, W. A., Manning, G., Irwin, C. R., and Lundy, F. T. (2013) LL-37 in periodontal health and disease and its susceptibility to degradation by proteinases present in gingival crevicular fluid. *J. Clin. Periodontol. 40*, 933−941.
(57) Tjabringa, S. G., Rabe, K. F., and Hiemstra, P. S. (2005) The human cathelicidin LL-37: a multifunctional peptide involved in infection and inflammation in the lung. *Pulm. Pharmacol. Ther. 18*, 321−327.
(58) Nan, Y. H., Bang, J.-K., Jacob, B., Park, I.-S., and Shin, S. Y. (2012) Prokaryotic selectivity and LPS-neutralizing activity of short antimicrobial peptides designed from the human antimicrobial peptide LL-37. *Peptides 35*, 239−247.

DOI: 10.1021/acs.biochem.5b00231
Biochemistry 2015, 54, 2785−2798